15th Seminar "New Trends in Research of Energetic Materials", Part II, pp. 790-799, ISBN 978-80-7395-480-2, University of Pardubice, Pardubice, Czech Republic, April 18–20, 2012.

Influence of local atmosphere characteristics to range of 155 mm M864 projectile

Sabina Serdarević-Kadić, Berko Zečević, Jasmin Terzić and Alan Ćatović

University of Sarajevo, Mechanical Engineering faculty, Bosnia and Herzegovina

e-mail: serdarevic@mef.unsa.ba

Abstract:

Projectiles with base bleed use concept of reducing base drag by injection gas generated by burning composite propellant, into the base area.

Influence of atmosphere characteristics at different geographic locations and positions of firing locations with respect to local conditions to drag coefficient of 155 mm M864 is studied by commercially CFD code FLUENT. The M864 projectile is chosen because there are many available experimental data.

Base bleed output mass flow rate depends on the chamber pressure, the pressure into which it exhausts, time and spin rate. Average injection parameter is estimated by mass of propellant and burning time. Ignition phase of propellant burn is taken into account..

Keywords: base bleed, mass flow rate, injection parameter

1 Introduction

The aerodynamic drag is one of the most important parameter in the design of the shell. The drag consists of three components: the pressure drag or wave drag (excluding the base), the viscous drag and the base drag. The biggest part of total drag is the base drag and it can be higher of 50% of total drag. The base drag depends on the pressure acting on the base and of the three drag components it is the most difficult to predict.

During projectile flight, region of underpressure is created behind the base of the projectile. The region leads to curve of streamlines to axis. Close to axis, streamlines have to curve again to be parallel with axis. The phenomenon is followed with shock waves and vortex. At the point of streamlines impact, overpressure zone is made and air is flowing from the zone to base of projectile and is filling vacuum on the base. Curved boundary layer extension pulls air from base of projectile. On this way recirculation region is made behind the base (figure 1a). Injecting small amounts of gas into the flow field behind the base of the projectile will split the originally large recirculation zone into two halves - one recirculation region remains at the symmetry axis (PRR), and the other one is formed right behind the base corner (SRR) (figure 1b.). As the mass flow rate is increased, the recirculation zone at the axis is pushed further out, and the other one at the base corner becomes larger. If the mass flow rate is increased away, the recirculation region near the axis disappears, and the base-bleed flow follows a straight path.

Projectiles with base bleed, therefore, use concept of reducing base drag by injection gas generated by burning composite propellant, into the base area. Composite propellant is housed in the afterbody of projectile. Base bleed output mass flow rate depends on the chamber pressure, the pressure into which it exhausts, time and spin rate.

Taking into account ignition time of propellant, authors are studied influence of atmosphere characteristics, at different geographic locations and positions of firing locations with respect to local conditions, to drag coefficient of projectile with base bleed by commercial CFD code FLUENT.

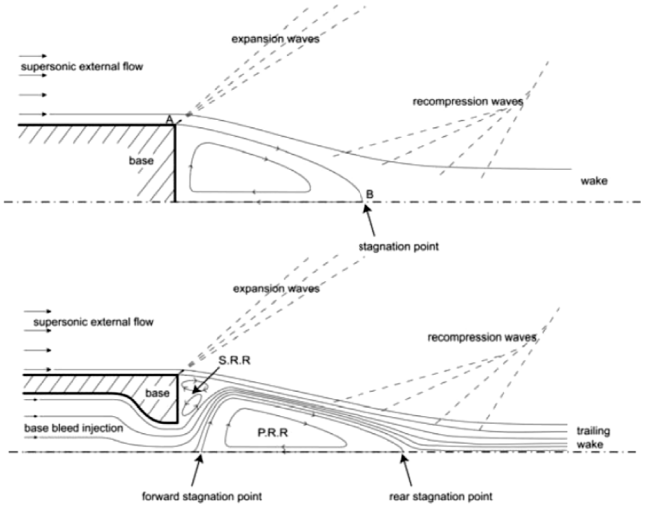

Figure 1: Flow field behind a projectile: a) without base bleed; b) with base bleed

2 Background literature

The technique is known as base bleed was a subject of experimental (Baker, Davis & Matthews, 1951.; Murthy et al. 1976; Murthy & Osborn, 1976,; Strahle, Hubbartt & Walterick, 1982.) and numerical (Sahu, Neitubicz & Steger, 1985.; Sahu 1986.) studies.

Application of approved numerical techniques to base bleed projectile configuration was started by Sahu. In the initial work, the author was considered projectile configuration without afterbody and with flat base and he was modeled injection of cold gas. As interest is extended to M864 projectile, „dome" effect of base and injection of hot gas to zone behind the projectile are researched by Neitubicz and Sahu (1988).

Extensive experimental investigations on 155 mm projectile M864 were made Kayser, Kuzan and Vasquez. They were measured pressure and temperature in base region during the projectile flight and time of base bleed burning while taking into account spin of projectile. Results of the experiments and computations are applied to develop an engineering model to compute the flight performance of the M864 base bleed projectile by Danberg (1990.).

Nietubicz and Gibeling (1995) are modeled the solid propellant combustion using the approach developed by Gibeling and Buggeln (1991) and the results are incorporated to Navier-Stokes code to simulate flow field in the base region of M864 projectile. Kaurinkoski (2000) is implemented eddy breakup model for chemical reactions to FINFLO solver and indicated the dramatic effect which chemical reactions have on the aerodynamic drag of a base-bleed projectile.

Base bleed projectile trajectory estimating by modified mass point model developed by Lieske is described in STANAG 4355. Drag coefficient corrections in functions of initial angle, spin, local air pressure and time of base bleed operating are made during exterior ballistic calculations.

There are significant numbers of reports about extended range projectile by base bleed, based on theoretical, experimental and numerical methods, but there are nothing about influence of geographic location and launching position with atmospheric parameters to drag coefficient of base bleed projectile.

2.1 Base bleed

It is customary when considering base bleed to define a nondimensional injection parameter I. The parameter is the ratio of the bleed mass flow rate, by the product of the base area, and the freestream mass flux :

$$I = \frac{\dot{m}_e}{\rho_\infty \cdot v_\infty \cdot A_{base}} \quad \textbf{(1)}$$

Combustion products bleed through orifice by subsonic velocity. From modified form of the incompressible Bernoulli equation along with the continuity equation, mass flow rate of combustion products at exit is:

$$\dot{m}_e = \left(C_v \cdot A_{orf} \sqrt{2 \cdot \rho_e \cdot P_e}\right) \cdot \sqrt{\frac{P_c}{P_e} - 1}\,. \quad \textbf{(2)}$$

where: ρ_e is density of combustion products at exit of orifice, C_v is discharge coefficient, A_{orf} is orifice area, P_e is exit pressure and P_c is chamber pressure.

The chamber pressure can be determined from mass balance law:

$$\dot{m}_p = \frac{dM}{dt} + \dot{m}_e\,. \quad \textbf{(3)}$$

Mass flow rate generated by propellant combustion is:

$$\dot{m}_p = \rho_p \cdot \dot{r} \cdot A_{burn} \quad \textbf{(4)}$$

where: ρ_p is propellant density, $\dot{r}$ is burn rate of propellant and A_{burn} - burning area.

Propellant burn rate depends of chamber pressure as described by Saint-Robert's law:

$$\dot{r} = a \cdot P_c^n \quad \textbf{(5)}$$

where: a is the burn rate coefficient, n is the pressure exponent and P_c is the combustion chamber pressure.

Mass of combustion product accumulated in chamber is:

$$M = \rho_g \cdot V \quad \textbf{(6)}$$

where: ρ_g is combustion products density in chamber and V is free volume of chamber.

Change of combustion products mass accumulated in chamber is very small, so mass balance equation can be written as:

$$\rho_p \cdot a \cdot P_c^n \cdot A_{burn} = \left(C_v \cdot A_{orf} \sqrt{2 \cdot \rho_e \cdot P_e}\right) \cdot \sqrt{\frac{P_c}{P_e} - 1} \quad \textbf{(7)}$$

2.2 Aerodynamic drag coefficient

It is assumed that mass injection into the near wake only affects the pressure distribution on the projectile base and thus only affects the base drag. Forebody pressure and viscous drag are unaffected.

The base drag component of a projectile is directly related to average projectile base pressure as follows:

$$C_{Db} = \frac{1 - \frac{P_b}{P}}{\frac{\gamma}{2} \cdot M^2 \cdot \frac{1}{d_b^2}} \quad \textbf{(8)}$$

where: d_b is base diameter of projectile in calibers, M is local flight Mach number, P is local atmospheric air pressure, P_b is average projectile base pressure and γ is ratio of specific heats.

From this relationship, theoretical difference in the base drag component for a projectile without non-operating base bleed (inert projectile), average base pressure P_{bi} and an operating base bleed, average base pressure P_{bb}, can be written as:

$$\Delta C_{D0_{bb}} = \frac{\frac{P_{bb}}{P} - \frac{P_{bi}}{P}}{\frac{\gamma}{2} \cdot M^2 \cdot \frac{1}{d_b^2}} \tag{9}$$

or

$$\Delta C_{D0_{bb}} = C_{D0} - C_{D0_{bb}} \tag{10}$$

C_{D0} - drag coefficient of inert projectile

$C_{D0_{bb}}$ - drag coefficient of projectile with base bleed operating

The difference in the average base pressure ratios is assumed in the form [6]:

$$\frac{P_{bb}}{P} - \frac{P_{bi}}{P} = I\left(\frac{\delta BP}{\delta I}\right) \tag{11}$$

where for low injection rates and a fixed gas temperature $\delta BP/\delta I$ is shown on figure 2. For the higher values of nondimensional injection parameters, $\delta BP/\delta I$ as function of Mach number for different values of parameter I on figure 3.

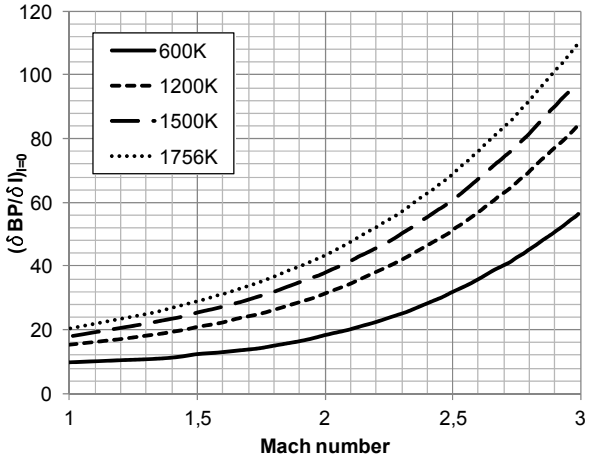

Figure 2: Change in base pressure for change in injection parameter vs. Mach number for low injection rates and various temperature

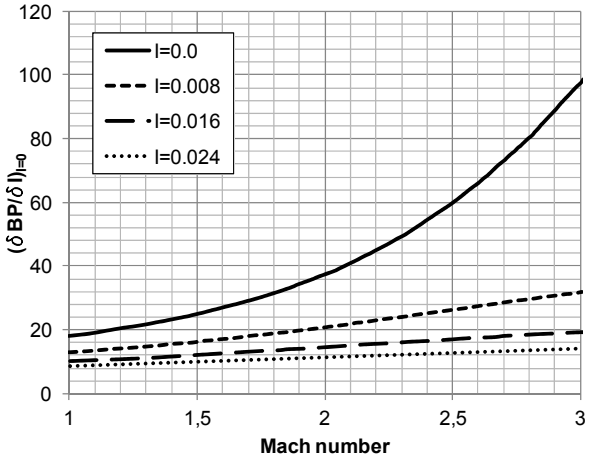

Figure 3: Change in base pressure for change in injection parameter vs. Mach number for various injection parameters and T = 1500K

3 Research and results analysis

In the work, research was done on the projectile M864 that incorporates base burn technology to increase its range. The projectile is a 155 mm, cargo-carrying projectile (Figure 4).

Extended range is achieved by using gas generator housing in the boat-tail of projectile. Gas generator consists of two identical solid propellant grains (Figure 5). These two elements provide an inner cylindrical burning surface and four planer surfaces separated by a 3 mm slot. The slot is held open during launch by four spacers. Solid propellant is inhibited at the surfaces adjacent to the base bleed case.

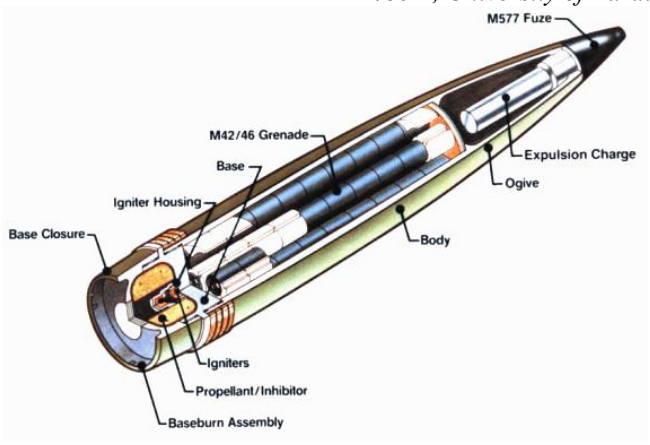

Figure 4: M864 Projectile

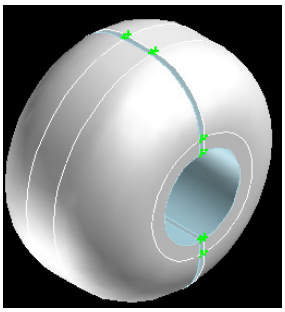

Figure 5: Propellant grain geometry

Change of burning area as function of the web is determined by graphical method and the results are shown in diagram $A_{burn}=A_{burn}\ (w)$ (Figure 6). The function $A_{cyl}=A_{cyl}\ (w)$ represents burning surface area of inner cylindrical surface, and the function $A_{slot}=A_{slot}\ (w)$ represents burning surface area of four planar surfaces.

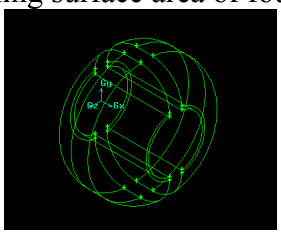

w = 5 mm

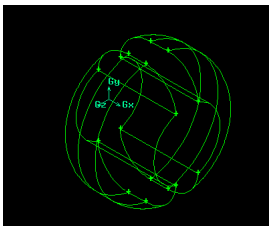

w = 20 mm

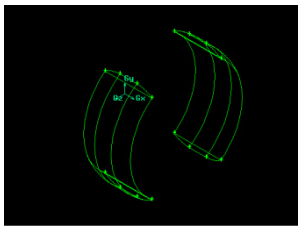

w = 35 mm

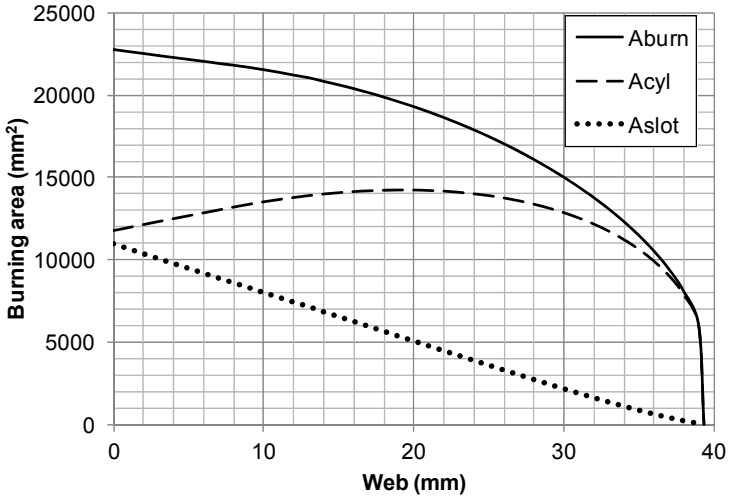

Figure 6: Grain burning surface areas as a function of web

Mass flow rate as a function of operating time of base bleed is determined by iterative method based on the known initial chamber pressure. The initial chamber pressure is assumed to be equal to ambient pressure in the moment when base bleed is started to work. Chamber temperature is assumed to be constant while base bleed is operating and equal 1500 K.

Ignition time of 0.5 second is assumed. Burn rate is determined separately for cylindrical surface and for planar surfaces, taking into account spin of projectile of 1550 rad/s [9]. Strand burn rate is taken from a work of Miller and Holmes [11]:

$$\dot{r} = 0.9132 \cdot P_c^{0.6655} \qquad \textbf{(12)}$$

The estimating strand burn rate should increase by 7% in order to obtain agreement with the ground based tests with zero spin.

Burn rate is determined separately for cylindrical surface $\dot{r}_c$ and for planar surfaces, $\dot{r}_s$:

$$\dot{r}_c = f_c(p)\cdot \dot{r}$$
$$\dot{r}_s = f_s(p)\cdot \dot{r} \quad \textbf{(13)}$$

where f_c and f_s are factors related to the spin rate (figure 7)

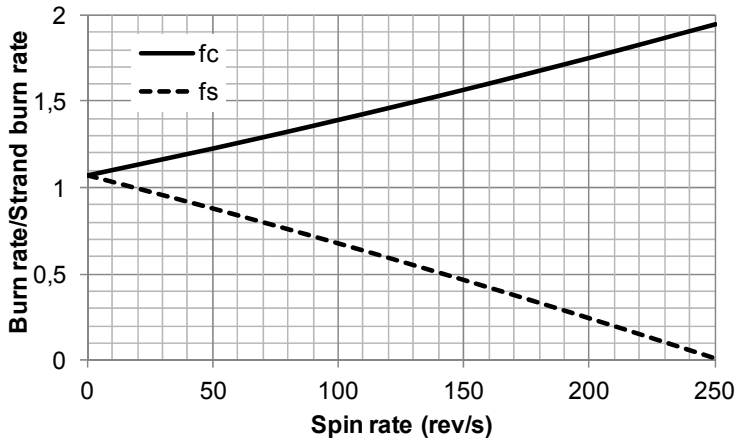

Figure 7: Effect of spin rate on burn rate for the cylindrical and slot surfaces [9]

3.1 Starting points for research

Three cases of launching are investigated. Four points on trajectory are chosen in the every case, the first point was corresponded to the beginning of base bleed operation and the other are related to selected velocities of projectile (M = 1.568, 1.305 and 1.2). Initial velocity was $V_0 = 806.6\ m/s$ and initial angle was $\theta_0 = 47.8°$.

For the first case, as reference, standard conditions are used. Projectile was launched from sea level with air pressure of $P = 101325\ Pa$ and air temperature of $T = 288.15\ K$ in the moment of launching.

For the second case, location in Europe is chosen, with altitude of $h = 511\ m$ and measured pressure and temperature were $P = 102100\ Pa$ and $T = 263.15\ K$.

For the third case, location in Africa is chosen, with altitude of $h = 31\ m$ and measured pressure and temperature were $P = 101600\ Pa$ and $T = 295.15\ K$.

Initial pressure of base bleed is calculated from the projectile position at the moment when base bleed starts to work for every case of launching.

In the first case, ambient air pressure was $P_\infty = 97842\ Pa$ at the moment when base bleed was started to operate, projectile velocity was $V = 784.3\frac{m}{s}$ and mass flow rate of bleeding combustion products was $\dot{m} = 0.0335557\frac{kg}{s}$.

In the second case, at the moment of starting base bleed, were calculated $P_\infty = 98553\ Pa$, $V = 782.9\frac{m}{s}$ and $\dot{m} = 0.033718\frac{kg}{s}$.

At the launching from the third location, calculating values were $P_\infty = 98105\ Pa$, $V = 784.6\frac{m}{s}$ and $\dot{m} = 0.0336157\frac{kg}{s}$.

Ambient conditions for selected velocities of projectile are determined from projectile altitude at the moment when projectile velocity is equal to selecting velocity. For the time of flight which is consistent with the desired velocity, keeping in mind initiation time, is estimated chamber pressure and mass flow rate from interior ballistics calculations.

For the other choosing projectile velocities, estimating mass flow rates of bleeding combustion products are shown in table 1.

Table 1: Mass flow rate vs. Mach number for selecting cases

$\dot{m}\ (\frac{kg}{s})$	M_∞		
	1.2	1.3	1.568
Case 1: Standard conditions, sea level	0.021991	0.0356428	0.042229
Case 2: Location in Europe	0.018675	0.0334685	0.042136
Case 3: Location in Africa	0.023092	0.0361060	0.042333

3.2 Numerical simulation of the flow field behind projectile

Gambit, preprocessor for CFD analysis, is used for constructing structured mesh around a projectile and inside the chamber of combustion. Mesh is consisted three blocks for inert projectile and four blocks for projectile with working base bleed. Changes to the block related to the chamber are made in function of burning area

Solution was done by using two dimensional axisymmetric density based solver with Splart - Allmaras viscous model and first order upwind discretization of flow equations.

Computing fluid mechanics enables visualization flow field around a projectile. Streamlines behind the base of projectile with and without hot gas injection for the first case are shown on figure 8.

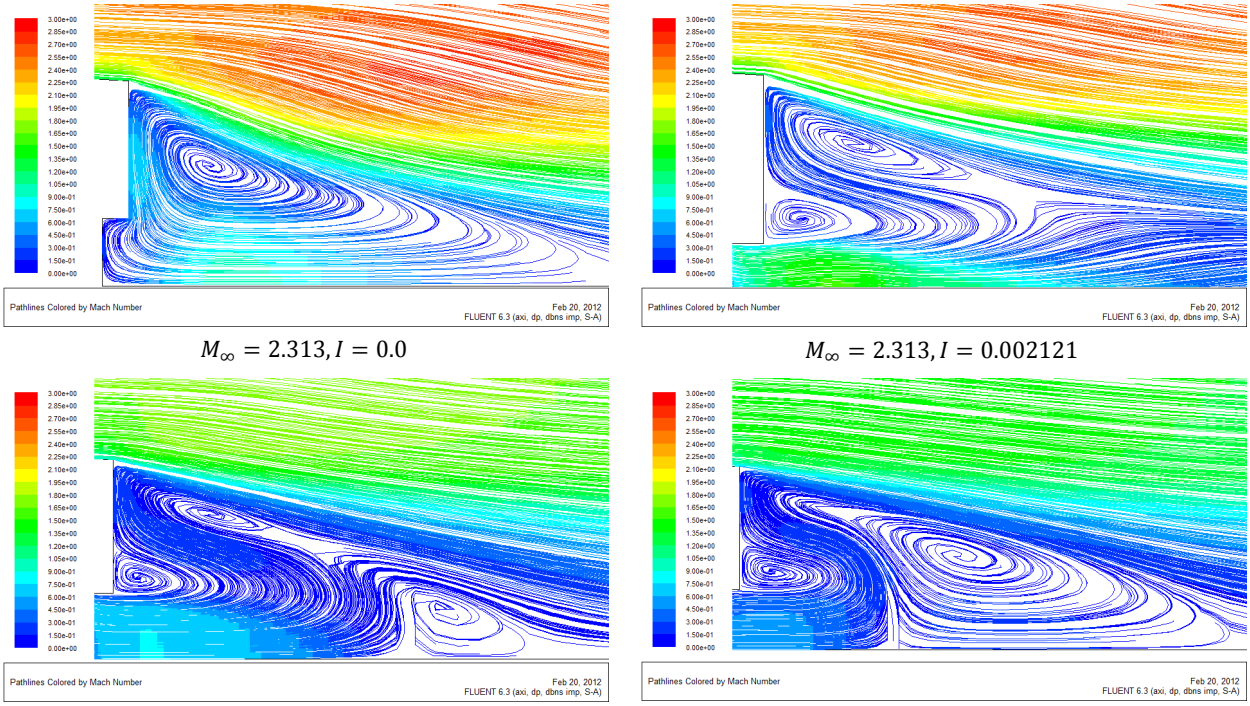

$M_\infty = 2.313, I = 0.0$ $M_\infty = 2.313, I = 0.002121$

$M_\infty = 1.568, I = 0.006569$ $M_\infty = 1.305, I = 0.008286$

Figure 8: Streamlines behind projectile as function of parameter *I* and Mach number for the first case

Changes of the nondimensional injection parameter related to launching locations and real atmospheric parameter as function of Mach number are shown on the diagram (figure 9). Nondimensional injection parameters for the first case are taken as reference values.

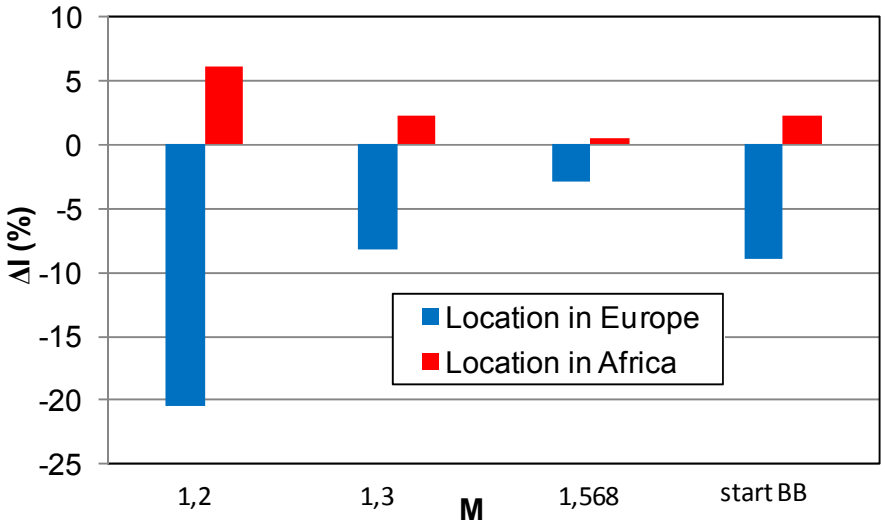

Figure 9: Changes of injection parameter for the different locations of launching in percentages

Launching location, from the point of pressure and temperature, influences to parameter *I* which reflects the more complex flow field behind base of projectile.

Reductions of drag coefficient by base bleed in the three cases related to drag coefficient of projectile with inert base bleed for the different Mach numbers are shown in table 2.

Table 2: Drag coefficient reduction expressed in percentages

ΔC_{D0bb} (%)	M_∞			
	1.2	1.3	1.568	0.5 second after launching
Case 1 h = 0 m; P = 101325 Pa; T = 288.15 K	3.46%	10.06%	6.29%	5.78% (M = 2.31)
Case 2 h = 511 m; P = 102100 Pa; T = 263.15 K	2.98%	5.69%	6.25%	4.39% (M = 2.416)
Case 3 h = 31 m; P = 101600 Pa;T = 295.15 K	2.96%	6.07%	6.28%	5.94% (M = 2.285)

Figure 10 shows drag coefficient of inert projectile determining by CFD simulation at tunnel conditions corresponding sea level and drag coefficients of base bleed projectile for every investigating case.

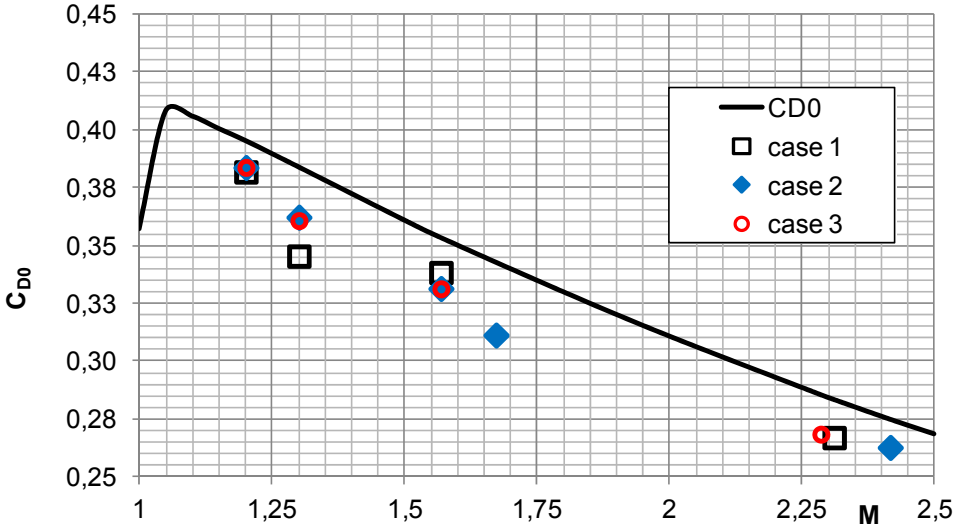

Figure 10: Drag coefficient as function of Mach number

These results are interesting because projectile spends the longest time in transonic and low supersonic region. The future investigation should be directed to the incorporation results of numerical simulation to 4DOF model of trajectory

4 Conclusion

In the work, authors are shown that location of launching (altitude, ambient pressure and temperature) influences to drag coefficient of projectile with base bleed.

We need to continue research on this subject through: increasing number of points, determining the parameter that have the greatest influence and finding a model that provides better accuracy for drag coefficients.

At the mixing subsonic and supersonic flow, flow equations in applied model are converged only with the first order upwind discretization. From this reason, drag coefficient of inert projectile determining with the same conditions was higher value.

References

[1] J. Sahu, C. J. Nietubicz, J. L. Steger: "Navier–Stokes Computations of Projectile Base Flow with and without Mass Injection", *AIAA Journal*, Vol. 23, No. 9, pp. 1348–1355, **1985.**

[2] J. Sahu, J. E. Danberg: "Navier–Stokes Computations of Transonic Flows with a Two-Equation Turbulence Model", *AIAA Journal*, Vol. 24, No. 11, pp. 1744–1751, **1986.**

[3] L. D. Kayser, J. D. Kuzan, D. N. Vazquez: "In Flight Pressure Measurements on Several 155mm, M864 Base Burn Projectiles", Report BRL-MR-3888, U.S. Army Ballistic Research Laboratory, Aberdeen Proving Ground, MD, **1991.**

[4] L. D. Kayser, J. D. Kuzan, D. N. Vazquez: "Flight Testing for a 155mm Base Burn Projectiles", Report BRL-MR-3830, U.S. Army Ballistic Research Laboratory, Aberdeen Proving Ground, MD, **1990.**

[5] P. Kaurinkoski: "Simulation of the Flow Past a Long-Range Artillery Projectile", Dissertation for the degree of Doctor of Science in Technology, Helsinki University of Technology, **2000.**

[6] R. F. Lieske, J. E. Danberg,: "Modified Point Mass Trajectory Simulation for Base-Burn Projectiles", Report BRL-TR-3321, U.S. Army Ballistic Research Laboratory, Aberdeen Proving Ground, MD, **1992.**

[7] C. J. Nietubicz, H. J. Gibeling:" Navier-Stokes Computations for a Reacting M864 Base Bleed Projectile", ARL-TR-875, U.S. Army Ballistic Research Laboratory, Aberdeen Proving Ground, MD, **1995.**

[8] STANAG 4355 - THE MODIFIED POINT MASS AND FIVE DEGREES OF FREEDOM TRAJECTORY MODELS, Brussels, Belgium, Edition 3, **2009.**

[9] J. E. Danberg: "Analysis of the Flight Performance of the 155 mm M864 Base Burn Projectile", Report BRL-TR-3083, U.S. Army Ballistic Research Laboratory, Aberdeen Proving Ground, MD, **1990.**

[10] H. J. Gibeling and R. C. Buggelin: "Reacting Flow Models for Navier-Stokes Analysis of Projectile Base Combustion", *AIAA Journal*, Paper 91-2077, Reston, VA, **1991.**

[11] M. S. Miller, H. E. Holmes:"An Experimental Determination of Subatmospheric Burning Rates and Critical Diameters for AP/HTPB Propellant", *Proceedings of the 1987 JANNAF Combustion Meeting*, Monterrey, California, **1987.**

[12] L. D. Kayser, J. D. Kuzan, D. N. Vazquez: "Ground Testing for Base Burn Projectile Systems", Report BRL-MR-3708, U.S. Army Ballistic Research Laboratory, Aberdeen Proving Ground, MD, **1988.**

[13] G. D. Catalano, W. B. Sturek: "A Numerical Investigation of Subsonic and Supersonic Flow Around Axisymmetric Bodies", Report ARL-TR-2595, Army Research Laboratory, Aberdeen Proving Ground, MD, **2001.**
[14] Fluent, Inc. FLUENT Version 6.3, Lebanon, NH, **2006.**
[15] Fluent, Inc. GAMBIT Version 2.4.6, Lebanon, NH, **2006.**